J. Fluid Mech. (1991), *vol.* 223, *pp.* 589–601
Printed in Great Britain

On localized solutions in nonlinear Faraday resonance

By E. W. LAEDKE AND K. H. SPATSCHEK
Institut für Theoretische Physik I, Heinrich-Heine-Universität Düsseldorf,
D-4000 Düsseldorf, Germany

(Received 25 September 1989 and in revised form 30 July 1990)

The dynamics of a nonlinear modulated cross-wave of resonant frequency ω_1 and carrier frequency $\omega \approx \omega_1$ is considered. The wave is excited in a long channel of width b that contains water of depth d, which is subjected to a vertical oscillation of frequency 2ω. As has been shown by Miles (1984*b*), the complex amplitude satisfies a cubic Schrödinger equation with weak damping and parametric driving. The stability of its solitary wave solution is considered here in various parameter regions. We find that in a certain regime the solitary wave is stable. Completely new is the result of instability outside this parameter regime. The instability has also been verified numerically. It is shown that the final stage of solitary wave instability is a cnoidal-wave-type solution.

1. Introduction

This investigation was stimulated by a recent paper by Miles (1984*b*) who succeeded in developing a theory for the standing solitary wave observed by Wu, Keolian & Rudnick (1984). The wave appears owing to Faraday resonance, in which standing waves are parametrically excited in a basin that is subjected to a vertical oscillation at a frequency approximately twice the natural frequency of the dominant cross-wave. For the details of the theory we refer to the original articles of Miles (1984*a*, *b*) and Larraza & Putterman (1984). We shall use the notation of Miles in this paper.

The basic result of Miles is the cubic nonlinear Schrödinger equation

$$\mathrm{i}(r_t+\alpha r)+Br_{XX}+(\beta+A|r|^2)\,r+\gamma r^*=0 \tag{1.1}$$

for the complex amplitude of the dominant cross-wave. Here, α is the linear damping ($\alpha>0$) and the terms βr and νr^* appear because of the vertical oscillation $z=a_0\cos 2\omega t$ in the gravitational field $-g\hat{z}$. Introducing a smallness parameter ϵ (which also characterizes the amplitude of the otherwise nonlinear oscillation), one defines

$$\gamma \equiv \frac{\omega^2 a_0}{\epsilon g} > 0 \tag{1.2}$$

and

$$\beta \equiv \frac{\omega^2-\omega_1^2}{2\epsilon\omega_1^2}. \tag{1.3}$$

The frequency ω approximates the natural frequency $\omega_1=(gk\tanh kd)^{\frac{1}{2}}$, where k is the carrier wavenumber. β can have either sign: for $kd\to\infty, \beta<0$ whereas for finite kd-values $\beta>0$ is possible. In addition, since

$$B \equiv T+kd(1-T^2), \tag{1.4}$$

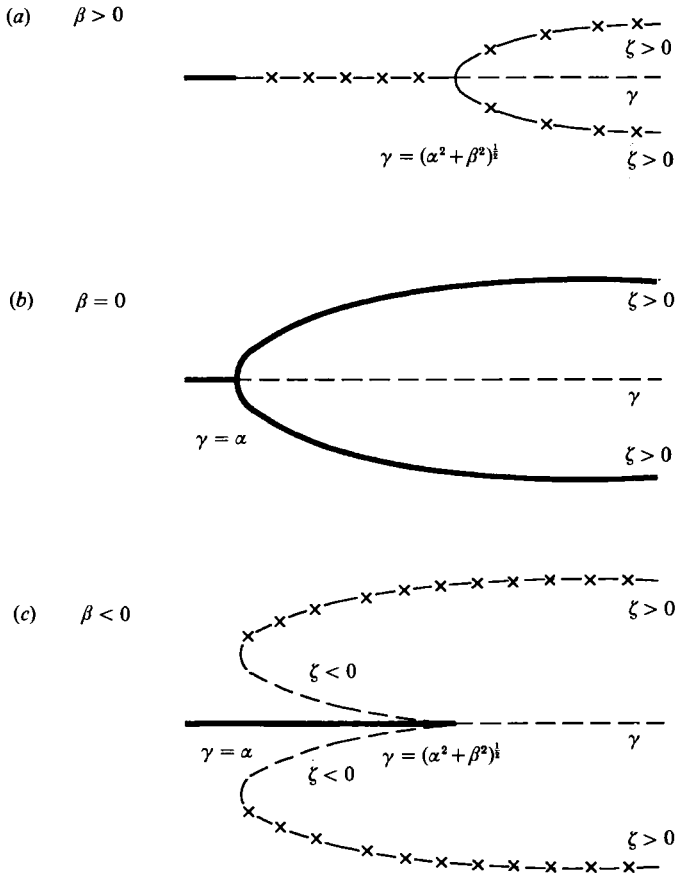

FIGURE 1. Bifurcation diagrams for X-independent stationary solutions for (*a*) $\beta > 0$, (*b*) $\beta = 0$, and (*c*) $\beta < 0$. Stable (——), unstable (– – – –), and modulationally unstable (— × — × — × —) branches can be recognized.

with $T \equiv \tanh kd$, we always have $B > 0$. On the other hand,

$$A \equiv \tfrac{1}{8}(6T^4 - 5T^2 + 16 - 9T^{-2}) \tag{1.5}$$

is a monotonically increasing function of kd with negative values for $T \to 0$, and $A \to 1$ for $T \to \pm 1$. Thus A can have either sign, but for solitary wave solutions $A > 0$ is required since $B > 0$. Without loss of generality in the following we set $A = B = 1$. By rescaling the amplitude, the X-coordinate, as well as α, β, and γ, we can always obtain this simplification for $A, B > 0$.

When looking for X-independent solutions we can summarize some well-known results. First $r \equiv 0$ is always a solution. For $\alpha/\gamma < 1$ (necessary condition) additional solutions $|r| \exp(i\varphi)$ can appear with

$$|r|^2 = -\beta \mp (\gamma^2 - \alpha^2)^{\frac{1}{2}} \tag{1.6}$$

and

$$\cos 2\varphi = \pm\left(1 - \frac{\alpha^2}{\gamma^2}\right)^{\frac{1}{2}}. \tag{1.7}$$

Thus, if $\beta < 0$ four solutions appear in the region $(\beta^2 + \alpha^2)^{\frac{1}{2}} > \gamma > \alpha$, and only two of

them remain for $\gamma > (\beta^2+\alpha^2)^{\frac{1}{2}}$. In the other case ($\beta \geqslant 0$), two X-independent solutions are always present for $\gamma > \alpha$. The situation is schematically shown in figure 1.

In that figure we have also included the stability results. The latter can be obtained in a straightforward manner within a linear stability analysis. We distinguish between stable, unstable, and modulationally unstable X-independent solutions. In our notation, stability and instability are first decided within a completely X-independent model. When the so-far stable solution becomes unstable with respect to X-dependent perturbations we call it modulationally unstable. To distinguish the various bifurcation branches it is advisable to introduce a new parameter

$$\zeta \equiv -\gamma \cos 2\varphi. \tag{1.8}$$

Using the latter, we find, for example, the instability criterion for the solution (1.6) and (1.7) in the form

$$\beta^2-[\kappa^2+\beta-2\zeta]^2 > 0, \tag{1.9}$$

where κ is the wavenumber of the (modulational) perturbations. From (1.6), i.e. $|r|^2 = -\beta+\zeta$, and (1.9) the corresponding conclusions summarized in figure 1 follow in a straightforward manner. Even simpler are the (in)stability arguments for the $|r| = 0$ solution. The rather trivial analysis leads to the instability criterion

$$\gamma^2-(\beta-\kappa^2)^2 > \alpha^2, \tag{1.10}$$

which completes the instability discussions for the X-independent solutions of (1.1). A final remark is appropriate with respect to the case $\beta = 0$. Note that for $\kappa \neq 0$ the two branches marked by $\zeta > 0$ correspond to a critical base in the sense of Lyapunov, where higher nonlinearities will determine the stability properties.

We continue this introductory part by posing the question of whether other X-independent solutions, i.e. limit cycles according to the Poincaré–Bendixson theorem (Guggenheimer & Holmes 1983), exist. Writing

$$r \equiv a+ib \tag{1.11}$$

we obtain from (1.1)

$$\dot{a} = -\alpha a-a^2b-b^3-\beta b+\gamma b, \tag{1.12}$$

$$\dot{b} = -\alpha b+ab^2+a^3+\beta a+\gamma a, \tag{1.13}$$

where the dot designates the time derivative. From these two equations obviously

$$\frac{\partial \dot{a}}{\partial a}+\frac{\partial \dot{b}}{\partial b} = -2\alpha < 0 \tag{1.14}$$

follows which, because of the logarithmic contraction for the area within a closed trajectory (Lichtenberg & Liebermann 1983; Miles 1984*b*), excludes the possibility of limit cycles.

One of the main conclusions of Miles (1984*b*) was that in the present system solitary waves can be parametrically excited. The existence of localized solutions was discussed and the bifurcation diagram was found. By some approximate stability method (Makhankov 1978; Whitham 1974) which we call the variation-of-action method (Laedke & Spatschek 1979) a completely stable solitary wave branch was predicted. As we shall elucidate in the next section, this soliton branch should be similar to the $\zeta > 0$ branches shown in figure 1.

In this paper we want to emphasize the following points: (i) An exact instability

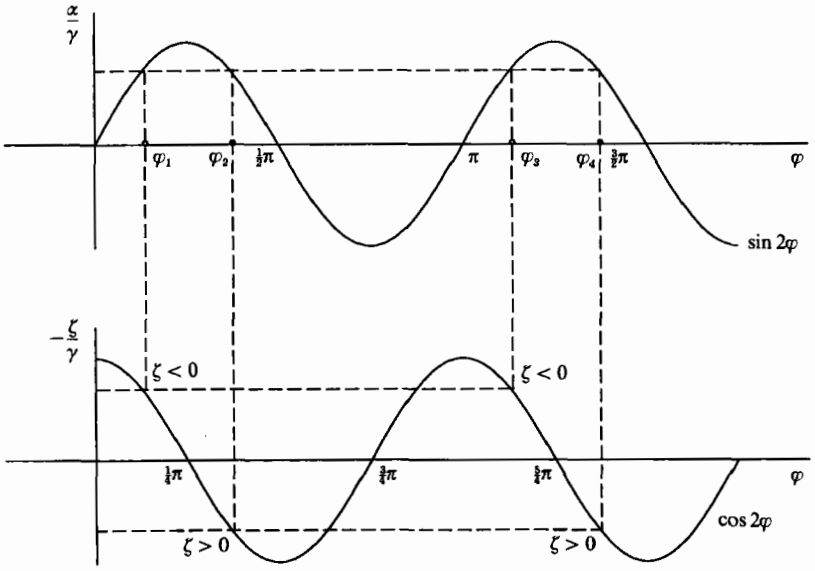

FIGURE 2. Construction of four possible phases at maximum from (1.8) and (2.3). Note that for $\beta \geqslant 0$ only the solutions φ_2 and φ_4, corresponding to $\zeta > 0$, are possible because of inequality (2.5).

calculation is possible in the region of interest. (ii) Existing solitary wave solutions are not stable in the whole parameter regime. (iii) An instability occurs which is expected to develop into a stable cnoidal-wave-type solution.

In order to demonstrate these conclusions, the paper is organized in the following way. In the next section we present the localized solitary wave solutions of (1.1). Their stability behaviour is analysed in §3 by variational principles. One special case cannot be treated by this method: its analysis is the main part of §4. All these analytical investigations are supplemented by a numerical solution of (1.1) in the relevant parameter regime. The numerics not only confirms the mathematical predictions; it also shows the nonlinear development of the instability which, at the present time, is beyond any analytical tractability.

2. Parametrically excited solitary waves

The non-trivial stationary solitary wave solutions of (1.1) (for $A = B = 1$), first presented by Miles (1984*b*), can be calculated in the following way. We substitute

$$r \equiv \psi_s(X) = G\,\mathrm{e}^{\mathrm{i}\varphi} \tag{2.1}$$

into (1.1) to obtain for G

$$\partial_X^2 G + G^3 + (\beta - \zeta)\, G = 0, \tag{2.2}$$

where ζ is as defined in (1.8). The imaginary part of (1.1) leads to the condition

$$\frac{\alpha}{\gamma} = \sin 2\varphi. \tag{2.3}$$

From (2.3) we immediately have the existence condition

$$\gamma > \alpha. \tag{2.4}$$

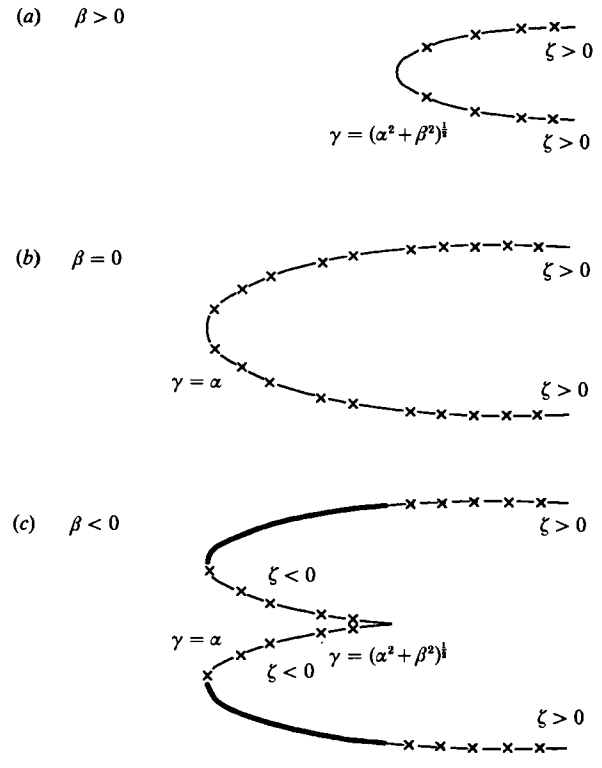

FIGURE 3. Bifurcation diagrams for solitary wave solutions. These should be compared to figure 1.

Demanding localized solutions of (2.2), the requirement

$$\beta < \zeta \tag{2.5}$$

is necessary. Then (2.2) has the well-known solitary wave solution

$$G = [2(\zeta-\beta)]^{\frac{1}{2}} \operatorname{sech}[(\zeta-\beta)^{\frac{1}{2}}X]. \tag{2.6}$$

Inequalities (2.4) and (2.5) lead to existence regions similar to those of the branches in figure 1 labelled by $\zeta > 0$ or $\zeta < 0$. Solutions of (1.8) and (2.3) are shown graphically in figure 2.

For $\beta \geqslant 0$ we have two principle solutions, whereas for $\beta < 0$ even four solutions are possible as long as inequality (2.5) is satisfied. The corresponding bifurcation diagrams are shown in figure 3 which should be compared to figure 1. The additional information contained in figure 3, i.e. the stability or the instability of the various branches, respectively, is not yet available. Its derivation is the contents of the following sections.

3. Instability by variational methods

We next perturb the solitary wave solution (2.1) in the form

$$r = (G+a+\mathrm{i}b)\,\mathrm{e}^{\mathrm{i}\varphi}, \tag{3.1}$$

to obtain the following dynamical equations for a and b:

$$\partial_t a = \mathrm{H}_+ b - 2\zeta b, \tag{3.2}$$

$$\partial_t b = -\mathrm{H}_- a - 2\alpha b. \tag{3.3}$$

Here, the Schrödinger operators

$$\mathrm{H}_+ \equiv -\partial_X^2 - G^2 + \zeta - \beta, \tag{3.4}$$

$$\mathrm{H}_- \equiv -\partial_X^2 - 3G^2 + \zeta - \beta \tag{3.5}$$

have been introduced. Their spectral properties are well-known: H_+ possesses the kernel function G, i.e.

$$\mathrm{H}_+ G = 0; \tag{3.6}$$

the continuum starts at $\eta^2 \equiv \zeta - \beta > 0$:

$$\mathrm{H}_+ \int^X G \,\mathrm{d}X' = \eta^2 \int^X G \,\mathrm{d}X'. \tag{3.7}$$

On the other hand, H_- has a negative eigenvalue,

$$\mathrm{H}_- G^2 = -3\eta^2 G^2, \tag{3.8}$$

and the kernel function $\partial_X G \equiv G_X \equiv \partial G/\partial X$, i.e.

$$\mathrm{H}_- \frac{\partial G}{\partial X} = 0. \tag{3.9}$$

For the following calculations it will be more appropriate to use

$$\mathrm{H} \equiv \mathrm{H}_+ - 2\zeta \tag{3.10}$$

instead of H_+. Then (3.2) is replaced by

$$\dot{a} = \mathrm{H}b. \tag{3.11}$$

We now summarize the basic properties of the Schrödinger operators H and H_-. For $\zeta < 0$, H is positive definite because of the property (3.6). In addition, H_- can be negative for even functions because (3.9) holds for an eigenfunction with one node. On the other hand, for $\zeta > 0$ the situation is different. H is negative for odd functions provided $\eta^2 - 2\zeta < 0$. This statement follows from the continuum limit (3.7). From the definition of $\eta^2 = \zeta - \beta$ we can write the latter condition in the form $\beta > -\zeta$. Thus for $\beta \geqslant 0$ the fact that H can be negative for odd functions is straightforward. In the case $\beta < 0$, we need the extra condition $\gamma^2 > \alpha^2 + \beta^2$ for a negative H. The operator H_- (for $\zeta > 0$) is positive definite for odd functions, being orthogonal to the kernel function G_X (see (3.9)).

These properties suggest combining (3.3) and (3.11) in the following forms:

(*a*) for $\zeta < 0$ $$\partial_t^2 a \equiv \ddot{a} = -\mathrm{H}\mathrm{H}_- a - 2\alpha\dot{a}, \tag{3.12}$$

(*b*) for $\zeta > 0$ $$\partial_t^2 b \equiv \ddot{b} = -\mathrm{H}_- \mathrm{H} b - 2\alpha\dot{b}. \tag{3.13}$$

On introducing $$\tilde{a} \equiv a\,\mathrm{e}^{\alpha t}, \tag{3.14}$$

and $$\tilde{b} \equiv b\,\mathrm{e}^{\alpha t}, \tag{3.15}$$

(3.12) and (3.13) become $$\ddot{\tilde{a}} = -\mathrm{H}\mathrm{H}_{-}\tilde{a} + \alpha^2\tilde{a}, \tag{3.16}$$

$$\ddot{\tilde{b}} = -\mathrm{H}_{-}\mathrm{H}\tilde{b} + \alpha^2\tilde{b}, \tag{3.17}$$

respectively. In the following we use (3.16) for $\zeta < 0$ and even perturbations $\tilde{a}$ and (3.17) for $\zeta > 0$ and odd functions $\tilde{b}$ in the subspace perpendicular to G_X, i.e.

$$\int \tilde{b} G_X \,\mathrm{d}X \equiv \langle \tilde{b} \,|\, G_X \rangle = 0. \tag{3.18}$$

With these restrictions both equations can be considered to be of the same type:

$$\ddot{\tilde{\varphi}} = -\mathrm{P}\mathrm{N}\tilde{\varphi} + \alpha^2\tilde{\varphi}, \tag{3.19}$$

where P is a positive operator and N has a negative eigenvalue. (For $\zeta < 0$: $\mathrm{P} \equiv \mathrm{H}$, $\mathrm{N} \equiv \mathrm{H}_{-}$, and the functions $\tilde{\varphi}$ are even. For $\zeta > 0$: $\mathrm{P} \equiv \mathrm{H}_{-}$, $\mathrm{N} \equiv \mathrm{H}$, and the functions $\tilde{\varphi}$ are odd and perpendicular to G_X, i.e. $\langle \tilde{\varphi} \,|\, G_X \rangle = 0$.) In Appendix A we discuss for the present case how a dynamical equation of the form (3.19) leads – with some restrictions for the test functions ψ – to the variational formulation (Blaha, Laedke & Spatschek 1987) for the exponential growth rate $\tilde{\Gamma}$,

$$\tilde{\Gamma}^2 = \alpha^2 + \sup_{\psi} \frac{-\langle \psi | \mathrm{N} | \psi \rangle}{\langle \psi | \mathrm{P}^{-1} | \psi \rangle}. \tag{3.20}$$

When applied to our original problem (3.12) and (3.13), we clearly find (for more details see Appendix B) that because of the transformations (3.14) and (3.15) formula (3.20) will predict instability for (i) $\zeta < 0$, as well as (ii) $\zeta > 0$ and $\beta > -\zeta$.

If we look at figure 3, we have thus proven (i) instability for the $\zeta < 0$ branches in all cases of β, and (ii) instability for the $\zeta > 0$ branches except for $\beta \leqslant 0$ in the region $\alpha^2 < \gamma^2 < \alpha^2 + \beta^2$. We have therefore to conclude that the parametrically excited solitary waves are not stable in the whole parameter regime. For example, for $\beta < 0$ and $\gamma^2 > \alpha^2 + \beta^2$ an instability occurs which, to the best of our knowledge, has not been discussed so far in the literature.

For the interpretation of that instability one cannot rely on the arguments for parametric instabilities of plane waves (see figure 1). If the physical picture for the latter were also to apply for solitary waves in general, the appearance of a stable solitary wave as shown in figures 3 and 4 would not be understandable.

4. Stability in the region $\beta < 0, \zeta > 0$, and $\alpha^2 < \gamma^2 < \alpha^2 + \beta^2$

Let us now consider the still-unsolved case of the existence of stable parametrically excited solitary waves in Faraday resonance. We demonstrate stability in the region $\beta < 0, \zeta > 0$, and $\alpha^2 < \gamma^2 < \alpha^2 + \beta^2$ in two ways: first by perturbation theory and secondly by numerics (see §5). In this section we present the simple but powerful perturbation scheme which has been successfully applied to other soliton problems by Zakharov, Kuznetsov & Rubenchik (1986).

Before going into the details of the calculation let us mention one important physical point. When comparing with the experimental results by Wu *et al.* (1984), we can recognize that upper and lower bounds for the driver amplitude are observed experimentally. They correspond to the limitation $\alpha^2 < \gamma^2 < \alpha^2 + \beta^2$. Furthermore,

when capillary effects are included (Miles 1984*a*), the region $\beta < 0$ effectively means $\omega < \omega_1(1+\sigma)^{\frac{1}{2}}$, where σ is the surface tension. Thus the right boundary of the driving frequency observed in the experiment also agrees with the predicted existence region $\beta < 0$ for stable solitary waves.

Let us consider the region $|\zeta| \ll |\beta|$ which can be realized by $\gamma \approx \alpha$ and $|\beta| \gg \alpha$. In this region, we rewrite (3.2) and (3.3) in the form

$$\partial_t a = \hat{\mathrm{H}}_+ b - \zeta b, \tag{4.1}$$

$$\partial_t b = -\hat{\mathrm{H}}_- a - \zeta a - 2\alpha b, \tag{4.2}$$

where

$$\hat{\mathrm{H}}_+ \equiv -\partial_X^2 - G^2 - \beta, \tag{4.3}$$

$$\hat{\mathrm{H}}_- \equiv -\partial_X^2 - 3G^2 - \beta. \tag{4.4}$$

The idea is to use $\partial_t \sim \Gamma$, $|\zeta|$, and α as small quantities. When combining (4.1) and (4.2) in the form

$$\partial_t^2 b = \Gamma^2 b = -(\hat{\mathrm{H}}_- + \zeta)(\hat{\mathrm{H}}_+ - \zeta) b - 2\alpha\Gamma b \tag{4.5}$$

we obtain at lowest order the equation

$$0 = -\hat{\mathrm{H}}_- \hat{\mathrm{H}}_+ b_0. \tag{4.6}$$

Its odd solution is

$$b_0 = \hat{\mathrm{H}}_+^{-1} G_X, \tag{4.7}$$

where G is given by (2.6) for $\zeta = 0$. Within the scaling $\Gamma^2 \sim |\zeta| \sim \alpha\Gamma \sim \epsilon^2$, where ϵ is a smallness parameter, we develop the perturbation series for $b = b_0 + \epsilon^2 b_2 + \ldots$. The contribution b_2 follows from

$$\Gamma^2 \hat{\mathrm{H}}_+^{-1} G_X = -\hat{\mathrm{H}}_- \hat{\mathrm{H}}_+ b_2 + \zeta \hat{\mathrm{H}}_- b_0 - \zeta G_X - 2\alpha\Gamma \hat{\mathrm{H}}_+^{-1} G_X; \tag{4.8}$$

this equation has the solvability condition

$$\Gamma^2 + 2\alpha\Gamma = -\zeta \frac{\langle G_X | G_X \rangle}{\langle G_X | \hat{\mathrm{H}}_+^{-1} | G_X \rangle}. \tag{4.9}$$

Note that

$$g \equiv \frac{\langle G_X | G_X \rangle}{\langle G_X | \hat{\mathrm{H}}_+^{-1} | G_X \rangle} > 0 \tag{4.10}$$

is a positive constant which can be evaluated without any difficulties. Thus the solution of (4.9),

$$\Gamma = -\alpha \pm (\alpha^2 - g\zeta)^{\frac{1}{2}}, \tag{4.11}$$

clearly tells us that (i) in accordance with the results of the previous section for $\zeta < 0$ an instability occurs, while (ii) for $\zeta > 0$ the stationary state is stable with respect to odd perturbations.

Let us now investigate the even solution

$$b_0 = G \tag{4.12}$$

of (4.6). Using the same scaling as in the previous case, we find instead of (4.8)

$$\Gamma^2 G = -\hat{\mathrm{H}}_- \hat{\mathrm{H}}_+ b_2 + \zeta \hat{\mathrm{H}}_- G - 2\alpha\Gamma G. \tag{4.13}$$

Its non-trivial solvability condition turns out to be

$$\Gamma^2 + 2\alpha\Gamma = \zeta \frac{\langle G | G \rangle}{\langle G | \hat{\mathrm{H}}_-^{-1} | G \rangle}. \tag{4.14}$$

Note that
$$g \equiv -\frac{\langle G|G\rangle}{\langle G|\hat{\mathrm{H}}_-^{-1}|G\rangle} > 0 \tag{4.15}$$

for the following reason. We have

$$\hat{\mathrm{H}}_-^{-1}G = -\frac{\partial G}{\partial(-\beta)} \tag{4.16}$$

and
$$\langle G|\hat{\mathrm{H}}_-^{-1}|G\rangle = -\frac{1}{2}\frac{\partial}{\partial(-\beta)}\langle G|G\rangle = -(-\beta)^{-\frac{1}{2}} < 0. \tag{4.17}$$

Thus, we again arrive at (4.11) and for $\zeta > 0$ the stability with respect to even perturbations follows.

We are aware of the fact that this is not a proof of stability for the whole region $\beta < 0, \zeta > 0$, and $\alpha^2 < \gamma^2 < \alpha^2+\beta^2$ in the strict mathematical sense. Going back to figure 3(*c*), we have just shown stability for the far left parts of the $\zeta > 0$ branches. Since we complete this investigation by a numerical procedure which clearly shows that (for $\beta < 0$) a transition from stable to unstable behaviour occurs in the $\zeta > 0$ branches at $\gamma = (\alpha^2+\beta^2)^{\frac{1}{2}}$ we do not aim here to construct a Lyapunov functional. Just to give the main idea of the latter procedure, we make the following remarks. One can prove that H is positive definite for odd functions whereas H_- is positive semidefinite for odd functions in the region being under consideration in this section. Thus, for odd functions a, multiply (3.12) by H^{-1} from the left in order to get a monotonically decreasing functional in time. The problem is that these considerations are restricted to odd functions whereas for even perturbations no successful procedure is known. We also shall not discuss the transition point from $\zeta < 0$ to $\zeta > 0$ which is a critical case in the sense of Lyapunov. It turns out that the critical case is nonlinearly unstable. It is straightforward to prove – starting from the basic equation (1.1) – that

$$\partial_t[(\mathrm{Re}\, r)^2 + (\mathrm{Im}\, r)^2] = \gamma(\mathrm{Im}\, r)^2. \tag{4.18}$$

Thus solutions with $\mathrm{Im}\, r \neq 0$ initially will grow.

5. Numerical manifestation of the analytical predictions

Equation (1.1) has been solved numerically by a nonlinear semi-implicit unitary Crank–Nicholson scheme (Spatschek *et al.* 1989). This allowed us (i) to test the stability predictions of §4; (ii) to verify the unstable behaviour in the complementary parameter regime, as pointed out in §3, and (iii) to look for the nonlinear development of an unstable solitary wave.

First, we investigated the parameter regime where stability is predicted. For $\beta < 0$ and $\zeta > 0$ several runs were performed in the region $\alpha^2 < \gamma^2 < \alpha^2+\beta^2$. All of them confirmed the analytical predictions. A typical result is shown in figure 4. Secondly, we took solitary wave solutions as initial conditions in the unstable parameter regime. As expected, they all became unstable within a finite time ($t \approx 20$). Finally, and most interesting, we followed the (nonlinear) time-development of an unstable solitary wave. Typical runs are shown in figures 5 and 6. At the first stage ($t \lesssim 50$) the breakup of the unstable soliton is clearly visible (figure 5). At a later time, a nice spatially coherent structure in space develops. It starts from the centre ($X = 0$) and spreads to larger X-values. It can be interpreted as a stable cnoidal wave (see figure 6).

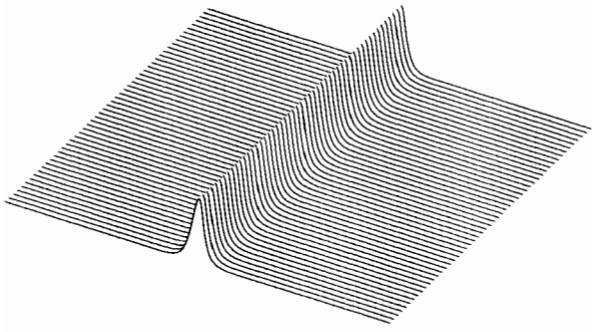

FIGURE 4. Space–time plot of a solitary wave (absolute value of the amplitude) for $\beta = -1, \alpha = 1$, $\gamma = 1.1$. The solitary wave is stable, at least for the time of computation ($0 \leqslant t < 100$).

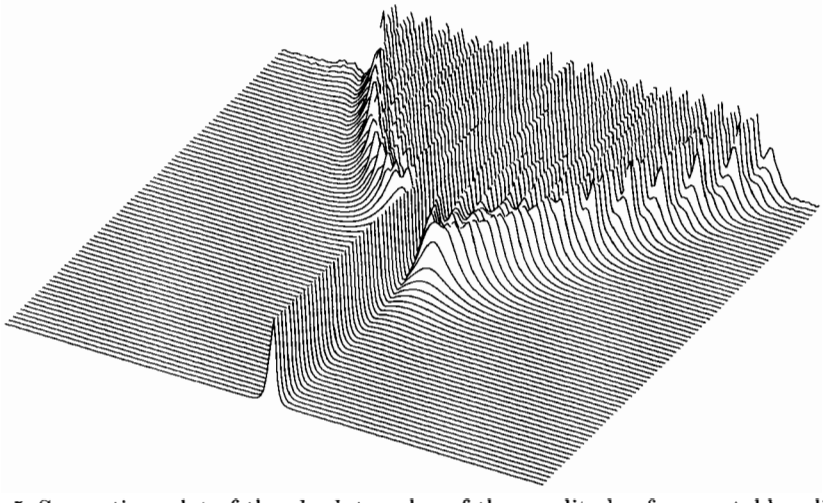

FIGURE 5. Space–time plot of the absolute value of the amplitude of an unstable solitary wave for $\beta = -1, \alpha = 1, \gamma = 1.6$. Initial phase of the instability for $-60 < X < 60$ and $0 < t < 75$.

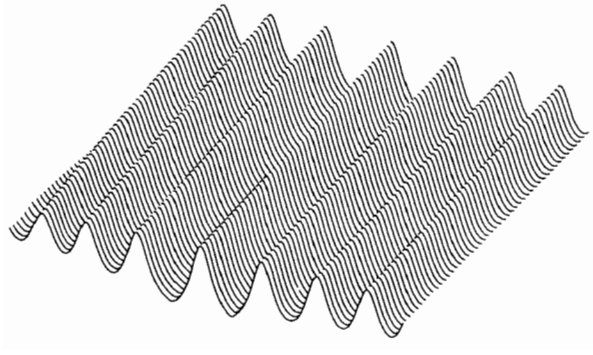

FIGURE 6. The same as figure 5 for large times and small X. A new state appears which can be interpreted as a cnoidal wave. Here the practically unchanged distribution for $-15 < X < 15$ is shown for the times $50 < t < 65$.

This work was supported by the Deutsche Forschungsgemeinschaft through SFB 237 and the Ministerium für Wissenschaft und Forschung des Landes Nordrhein-Westfalen. Discussions with Dr Funakoshi are gratefully acknowledged.

Appendix A. A variational principle for (3.19)

Since P is a positive operator, we rewrite (3.19) in the form

$$\mathrm{P}^{-1}\ddot{\tilde{\varphi}} = -(\mathrm{N}-\alpha^2\mathrm{P}^{-1})\tilde{\varphi}, \tag{A 1}$$

where the operator

$$\mathrm{F} \equiv -(\mathrm{N}-\alpha^2\mathrm{P}^{-1}) \tag{A 2}$$

is also positive. Multiplying

$$\mathrm{P}^{-1}\ddot{\tilde{\varphi}} = \mathrm{F}\tilde{\varphi} \tag{A 3}$$

from the left by $\dot{\tilde{\varphi}}$ and integrating over space we find

$$\langle\dot{\tilde{\varphi}}|\,\mathrm{P}^{-1}|\dot{\tilde{\varphi}}\rangle = \langle\tilde{\varphi}|\,\mathrm{F}|\tilde{\varphi}\rangle + \text{const.} \tag{A 4}$$

The constant of (time-) integration can be set to zero if we choose appropriate initial conditions, i.e. at $t = 0$ we demand $\dot{\tilde{\varphi}} = \tilde{\Gamma}\tilde{\varphi}$. Since F is positive, the constant $\tilde{\Gamma}$ follows without problems from

$$\tilde{\Gamma}^2 = \frac{\langle\tilde{\varphi}_0|\mathrm{F}|\tilde{\varphi}_0\rangle}{\langle\tilde{\varphi}_0|\mathrm{P}^{-1}|\tilde{\varphi}_0\rangle}, \tag{A 5}$$

where $\tilde{\varphi}_0$ is the initial distribution.

Also multiplying (A 1) from the left by $\tilde{\varphi}$ and integrating over space leads to

$$\langle\tilde{\varphi}|\mathrm{P}^{-1}|\ddot{\tilde{\varphi}}\rangle = \langle\tilde{\varphi}|\mathrm{F}|\tilde{\varphi}\rangle. \tag{A 6}$$

Since all the operators are self-adjoint, we can combine (A 4) and (A 6) to give

$$\partial_t^2 L = 2\langle\tilde{\varphi}|\mathrm{F}|\,\tilde{\varphi}\rangle, \tag{A 7}$$

where

$$L \equiv \tfrac{1}{2}\langle\tilde{\varphi}|\mathrm{F}|\,\tilde{\varphi}\rangle. \tag{A 8}$$

The following rearrangement using the Schwarz inequality,

$$\partial_t^2 L = 2\langle\dot{\tilde{\varphi}}|\mathrm{P}^{-1}|\dot{\tilde{\varphi}}\rangle = \frac{2\langle\dot{\tilde{\varphi}}|\mathrm{P}^{-1}|\dot{\tilde{\varphi}}\rangle\langle\tilde{\varphi}|\mathrm{P}^{-1}|\tilde{\varphi}\rangle}{\langle\tilde{\varphi}|\mathrm{P}^{-1}|\tilde{\varphi}\rangle} \geqslant 2\frac{\langle\dot{\tilde{\varphi}}|\mathrm{P}^{-1}|\tilde{\varphi}\rangle^2}{\langle\tilde{\varphi}|\mathrm{P}^{-1}|\tilde{\varphi}\rangle}, \tag{A 9}$$

proves the result

$$\partial_t\left(\frac{\partial_t L}{L}\right) \geqslant 0. \tag{A 10}$$

It has the solution

$$L \geqslant L_0\,\mathrm{e}^{\tilde{\Gamma}t}. \tag{A 11}$$

Since P and P^{-1} are positive operators, unstable perturbations exist with exponential growth rate $\tilde{\Gamma}$. Going back to (A 5) we can maximize with respect to the initial distributions to obtain the largest exponential growth rate:

$$0 < \tilde{\Gamma}^2 \leqslant \sup_{\psi}\frac{\langle\psi|\mathrm{F}|\,\psi\rangle}{\langle\psi|\mathrm{P}^{-1}|\,\psi\rangle}. \tag{A 12}$$

When we use the definition (A 2), (3.20) follows. It should be mentioned that the right-hand side of inequality (A 12) actually represents the maximum exponential growth rate.

Appendix B. Growth rates in the unstable cases

In §3 we have argued that all the unstable cases lead to equations of the type (3.19) with the result (3.20). A few additional remarks are necessary since we have subsidiary conditions to obey. Let us start with $\zeta > 0$ when we use (3.17), i.e.

$$\ddot{\tilde{b}} = -\mathrm{H}_- \mathrm{H}\tilde{b} + \alpha^2 \tilde{b}. \tag{B 1}$$

Let us restrict $\tilde{b}$ to odd functions with $\langle \tilde{b} \,|\, G_X \rangle = 0$, so that H_- is positive definite. As discussed already, H is negative in the region of interest $\gamma^2 > \alpha^2 + \beta^2$. For the second-order differential equation (B 1) we start with

$$\langle \tilde{b} \,|\, G_X \rangle_{t=0} = \langle \dot{\tilde{b}} \,|\, G_X \rangle_{t=0} = 0. \tag{B 2}$$

Then the differential equation (B 1) and (3.9) tell us that $\langle \tilde{b} \,|\, G_X \rangle$ remains zero in time. Thus we can use $\langle \tilde{\varphi} \,|\, G_x \rangle = 0$ as a consistent subsidiary condition for all times. Next, we have to say a few words about the inversion procedure applied in (A 1). Of course, we can always add an arbitrary function from the kernel of $\mathrm{P} \equiv \mathrm{H}_-$, i.e. (A 1) reads in the present case

$$\mathrm{H}_-^{-1} \ddot{\tilde{b}} = -\mathrm{H}\tilde{b} + \alpha^2 \mathrm{H}_-^{-1} \tilde{b} + \mu G_X. \tag{B 3}$$

Here μ is a free parameter. We fix it, however, by the requirement that we remain in the subspace orthogonal to G_X. Thus

$$\mu = \frac{\langle G_X | \mathrm{H} | \tilde{b} \rangle}{\langle G_X \,|\, G_X \rangle}. \tag{B 4}$$

The rest follows along the lines outlined in Appendix A. The maximum growth rate for $\zeta > 0$ in the region $\gamma^2 > \alpha^2 + \beta^2$ is

$$\tilde{\Gamma}^2 \equiv (\Gamma + \alpha)^2 = \alpha^2 + \sup_{\substack{\psi \text{ odd} \\ \langle \psi \,|\, G_X \rangle = 0}} \frac{-\langle \psi | \mathrm{H} | \psi \rangle}{\langle \psi | \mathrm{H}_-^{-1} | \psi \rangle}. \tag{B 5}$$

On the other hand, for $\zeta < 0$ a similar calculation leads to

$$\tilde{\Gamma}^2 \equiv (\Gamma + \alpha)^2 + \sup_{\psi \text{ even}} \frac{-\langle \psi | \mathrm{H}_- | \psi \rangle}{\langle \psi | \mathrm{H}^{-1} | \psi \rangle}, \tag{B 6}$$

when (3.16) is used. Both formulae prove the instability results summarized in §3.

REFERENCES

Blaha, R., Laedke, E. W. & Spatschek, K. H. 1987 Maximum growth rates for packets of waves in water of finite depth. *Phys. Fluids* **30**, 264–266.

Guggenheimer, J. & Holmes, P. H. 1983 *Nonlinear Oscillations, Dynamical Systems, and Bifurcations of Vector fields*. Springer.

Laedke, E. W. & Spatschek, K. H. 1979 On the applicability of the variation of action method to some one-field solitons. *J. Math. Phys.* **20**, 1838–1841.

Larraza, A. & Puttermann, S. 1984 Theory of non-propagating surface-wave solitons. *J. Fluid Mech.* **148**, 443–449.

Lichtenberg, A. J. & Lieberman, M. A. 1983 *Regular and Stochastic Motion*, p. 383. Springer.

Makhankov, V. G. 1978 Dynamics of of classical solitons. *Phys. Rep.* **35**, 1–128.

Miles, J. W. 1984*a* Nonlinear Faraday resonance. *J. Fluid Mech.* **146**, 285–302.

Miles, J. W. 1984*b* Parametrically excited solitary waves. *J. Fluid Mech.* **148**, 451–460.

SPATSCHEK, K. H., PIETSCH, H., LAEDKE, E. W. & EICKERMANN, TH. 1989 On the role of soliton solutions in temporal chaos: examples for plasmas and related systems. In *Singular Behavior and Nonlinear Dynamics*, pp. 555–564. World Scientific.

WHITHAM, G. B. 1974 *Linear and Nonlinear Waves*, pp. 601–603. Wiley.

WU, J., KEOLIAN, R. & RUDNICK, I. 1984 Observation of a non-propagating hydrodynamic soliton. *Phys. Rev. Lett.* **52**, 1421–1424.

ZAKHAROV, V. E., KUZNETSOV, E. A. & RUBENCHIK, A. M. 1986 Soliton stability. In *Solitons*, pp. 503–554. Elsevier.